Met. Mater. Int., Vol. 16, No. 2 (2010), pp. 339~347
doi: 10.1007/s12540-010-0427-7 Published 26 April 2010

Rigid-Plastic and Elastic-Plastic Finite Element Analysis on the Clinching Joint Process of Thin Metal Sheets

Vishara Jayasekara[1], Kyung Ho Min[1], Jeong Hoon Noh[1], Min Tae Kim[1], Jeong Min Seo[1], Ho Yong Lee[2], and Beong Bok Hwang[1,*]

[1] Department of Mechanical Engineering, Inha University, 253 Yong Hyun-Dong, Nam-Ku, Inchon 402-751, Korea
[2] Department of Mechanical Engineering, Dongguk University, 3ga 26, Pil-dong, Choong-gu, Seoul 100-715, Korea

(received date: 9 June 2009 / accepted date: 24 July 2009)

This article describes the joining of thin metal sheets by a single stroke clinching process. Elastic-plastic and rigid-plastic finite element analysis were applied by employing Coulomb friction and constant shear friction in order to investigate the behavior of the clinch joint formation process. Four process variables, such as die diameter, die depth, groove width, and groove corner radius were selected to investigate the parametric effect on the clinch joint. The strength of clinch joints were evaluated by examining the separation strengths, such as peel strength and tensile shear strength, respectively. A failure diagram was constructed that summarizes the analysis results. The simulation results showed that die diameter and depth were the most decisive parameters for controlling the quality of the clinch joint, while the bottom's thickness was the most important evaluation parameter to determine the separation strengths.

Keywords: clinching, alloys, joining, plasticity, computer simulation

1. INTRODUCTION

Clinching is a mechanical fastening technique performed at a rapid pace that joins thin sheets of metal by a combination of drawing and forming without thermal effects [1]. Clinching is a viable substitute for traditional joining techniques, such as screws, rivets and spot welding. Unlike conventional fastening methods, it does not require pre-formed holes, auxiliary material, or additional elements. Clinching equipment includes a tooling set with a punch and die. With the clinching process, similar-dissimilar or coated multiple layers of ductile sheet metals can be joined with a total thickness of 0.1 mm to 10 mm [2]. Clinching is mainly intended for sheet metal less than 3 mm of thickness, though it is most commonly used for wo layers. There are two different types of clinch joints, which are lanced lock (shear clinching) and press clinch (button or round clinch) [3]. The press clinch joint is often preferred due to its neat appearance and leak resistance. Press clinch joints can be formed with either single stroke clinching (displacement controlled) or double stroke clinching (force controlled) [4]. Single stroke clinching can be classified into different types of processes and its characteristics, which are known as divisible style die clinch, straight wall style solid die clinch, single punch clinch, flat point clinch, and plank clinch, respectively [5].

In recent years, the importance of mechanical joining techniques based on cold forming has been recognized due to its low cost and ease of automation. The clinching process has been implemented on light-weight structures with high production rates, such as automobiles, electronics, and household appliances. For instance, clinching is widely applied in the automobile industry since the sheets of material are generally not pierced for vehicle body applications [6,7]. It has been found that the joint strength depends on various geometrical process parameters [8]. The determination of process parameters have not yet been standardized for clinch joints, and therefore, different tool combinations have been used in the past to determine parameters [9]. Due to the necessity to provide guidelines for determining clinching process parameters, a finite element method is proposed in this study. As clinch joints are generated by overlapping metal sheets and deforming plastically by the drawing and forming, this process falls under the boundaries of elastic-plastic and rigid-plastic FE analysis methods. Also, considering sheet metals that have large deformation, Coulomb

*Corresponding author: bbhwang@inha.ac.kr

friction and constant shear friction can be employed between contact boundaries. Also, considering deformation of sheet metals, Coulomb friction or constant shear friction can be employed between contact boundaries, as joining process involves large deformation.

In the present study, an AA 5754 aluminum alloy was used for investigating the effect of different material models in the FE analysis of clinch joints. A forming process was simulated and numerically analyzed by rigid-plastic and elastic-plastic finite element methods that employed Coulomb friction and constant shear friction models, respectively. The die diameter D_d, die depth H, groove width w, and groove corner radius R_2 were observed in order to investigate the parametric effect on the forming process of the clinch joint. The peel-strengths and tensile shear strengths that resisted separation were evaluated for the quality of the clinch joint. The thickness of the undercut and the neck's bottom were examined after the process in order to identify failure modes and to draw a failure diagram. Thicknesses of undercut u, necks N_1, N_2, and bottoms X were examined and recorded after the process in order to identify failure modes and to draw failure diagram.

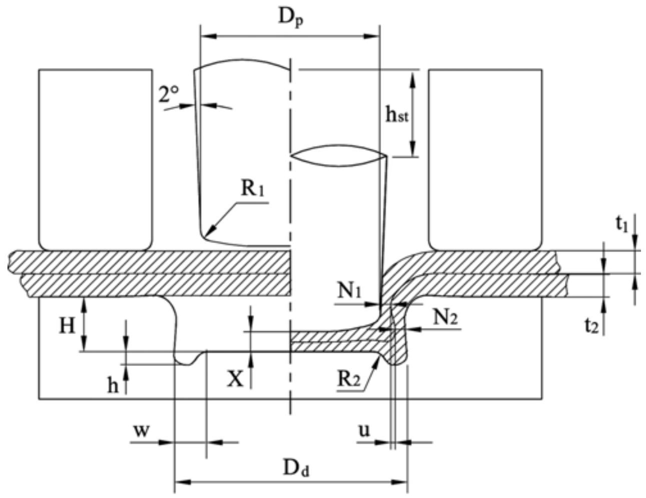

R_1 : punch corner radius
R_2 : groove corner radius
D_p : punch diameter
D_d : die diameter
H : die depth
X : Bottom thickness
u : Undercut
h : groove depth
w : groove width
t_1 : punch side sheet thickness
t_2 : die side sheet thickness
h_{st} : punch stroke
N_1 : Neck 1
N_2 : Neck 2

Fig. 1. Geometrical process parameters.

2. ANALYSIS BY FEM

2.1. Simulation Procedures and Process Parameters

The numerical simulation based on finite element methods offers an opportunity to explore the mechanism of the clinching process. Several methods may be applied to the finite element analysis of the clinching processes, e.g. elastic-plastic method [10-12] and rigid-plastic method [10,13,14,15]. Since the clinch joints are generated by overlapping metal sheets and are plastically deforming due to the punching and squeezing the area of the joint can produce large strain due to severe deformation. Therefore, the clinching process can be modeled as rigid-plastic by neglecting the elastic strains, which consequently make use of the rigid-plastic constitutive equation for computational economy and efficiency. It can also be modeled as elastic-plastic considering the elastic spring back effects of the sheet metals. The simulation results also depend on the friction model applied to the contact boundaries, the hardening properties of the sheets, and the geometry of the tools and sheets. The magnitude of frictional stresses are generally characterized in two ways: 1) Coulomb friction model, in which the magnitude of friction is proportional to the stress that is normal to the surface (contact pressure) and 2) the constant shear friction model, in which the interface friction is calculated by a constant fraction of the shear strength of the deforming body. Generally, Coulomb friction is used for the sheet metal forming process while constant shear friction is used for the large deformation process, respectively. The clinching process has a sheet metal forming large deformation. In this study, two different friction models were applied to simulate the clinching process in order to investigate how the friction model influences the simulation results and to see the differences. As sheet metal involves large deformation in clinching two different friction models were applied to simulate the clinching process in order to investigate how the riction model influences the simulation results and to see the differences. A commercially available finite element analysis program, Deform-2D™ [16], was used for modeling the process as an axisymmetric forming operation.

Figure 1 shows the geometry of the tooling and process parameters for the clinching process. Based on previous studies [13,17], the basic shape of tools, such as die diameter D_d, die depth H, groove width w, and groove corner radius R_2 were selected as the major process parameters that would influence the forming characteristics of the clinch joints. All of the specific values of the geometrical parameters used in the simulations are summarized in Table 1. The clinching die and punch were assumed as rigid bodies while the punch moved downward until the sheet material filled the die cavity completely.

AA 5754 aluminum alloy is widely used for automotive structural components because its formable nature, strength, and density [18]. It was selected as the model material in this study that focused on the simulations of the clinching process. Both the constant shear friction and Coulomb friction models were adopted in the analysis. A frictional factor of m

Table 1. Process parameters

Parameters	Values
Punch diameter (D_p)	5.0 mm
Punch corner radius (R_1)	0.2 mm
Draft angle of punch	2°
Die diameter (D_d)	5.6 mm, 6.0 mm, 6.4 mm
Die depth (H)	1.0 mm, 1.2 mm, 1.5 mm
Groove depth (h)	0.6 mm
Groove width (w)	0.6 mm, 0.8 mm, 1.2 mm
Groove corner radius (R_2)	0.1 mm, 0.3 mm, 0.5 mm
Frictional coefficient (μ)	0.12
Frictional factor (m)	0.12
Thickness punch side sheet (t_1)	0.5 mm
Thickness die side sheet (t_2)	0.5 mm
Stroke (h_{st})	until die cavity completely fills
Material	AA5754 aluminum alloy
Young's modulus (GPa)	70
Poisson's ratio (ν)	0.33
Flow stress (MPa)	$\bar{\sigma} = 250\bar{\varepsilon}^{0.3}$

= 0.12 and a frictional coefficient of μ = 0.12 were assumed for the sheets and tools [12,19].

2.2. Joint Strength and Evaluation Parameters

The strength of the clinch joints were analyzed to ensure and evaluate the quality of joints by simulating the peel tension and tensile shear tests, as shown in Figs. 2(a) and (b) respectively [20]. A commercially available FEM program Deform-3D™ [21] was used for this analysis and a 3D mesh was extrapolated with final process conditions from the 2D mesh employed in the Deform 2D to analyze the clinch joints. Simulations for both peel-tension and tensile-shear tests were executed under a displacement control condition, such that the top sheet kept separating from the fixed bottom sheet at a constant velocity. The same frictional conditions were used as above. In the peel tests, the top sheet separated from the bottom sheet at a constant velocity of 0.1 mm/s, which was applied 7.5 mm away from the center of the joint. In the tensile shear strength tests, the top sheet was pulled away from the bottom sheet at a constant velocity of 0.1 mm/s, which was tangent to the sheet surface.

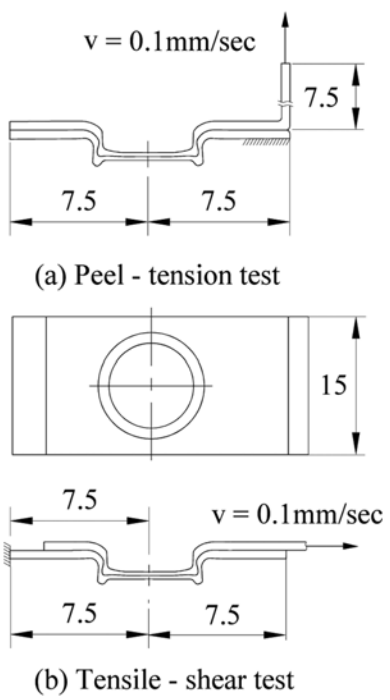

Fig. 2. Schematic test methods for separation strengths.

The quality of the clinching process can be evaluated by different parameters, for example, the static and fatigue strength of the joint, the corrosion resistance of the joints, or the visual appearance of the joint [22]. The joint strength was found to have varied with joining conditions, such as sheet thickness, punch diameter, and other process parameters. The optimum joining condition of the clinch joint under complex loading can be determined by correlating the strength ratio with the diameter ratio and sheet thickness ratio [8]. Since the clinching process is essentially a cold deformation of the overlapping sheets or profiles, and the material has geometrically changed in comparison to the original flat sheet metal, the joint quality can be monitored by measuring the bottom thickness of the joint known as the "X parameter", which is also called the ST-value, through the bottom width or diameter [4,23,24]. These monitoring techniques of clinch joints have a considerable advantage in that they are non destructive, in contrast to a spot weld joint or a screw assembly that cannot be checked for quality without destroying the assembled structure. The clinching joint is considered ideal if the die is filled fully with material, the sheets are completely connected together, there is no excessive stretching of the top sheet at the neck of the joint, and there is no counter piping [1].

3. RESULTS AND DISCUSSION

3.1. Flow patterns for different FE and friction models

Figure 3 illustrates a set of simulation results for the finite element model that retraces the forming chronology of the clinching process. Also, Fig. 3 represents the material flow and deformation patterns in terms of the direction and magnitude of flow velocities at selected forming stages of drawing, forming, and inverse extrusion, where a reduction in the bottom thicknesses (X) are 10%, 40% , and 60% of the total sheet thickness.

For the elastic-plastic FE models (Figs. 3(a) and (b)), in the beginning of the process where the bottom thickness (X) is 90 % of total sheet thickness, the outer periphery that was under the blank holder of the top sheet tended to flow into the die and the bottom sheet flew outward. However, the

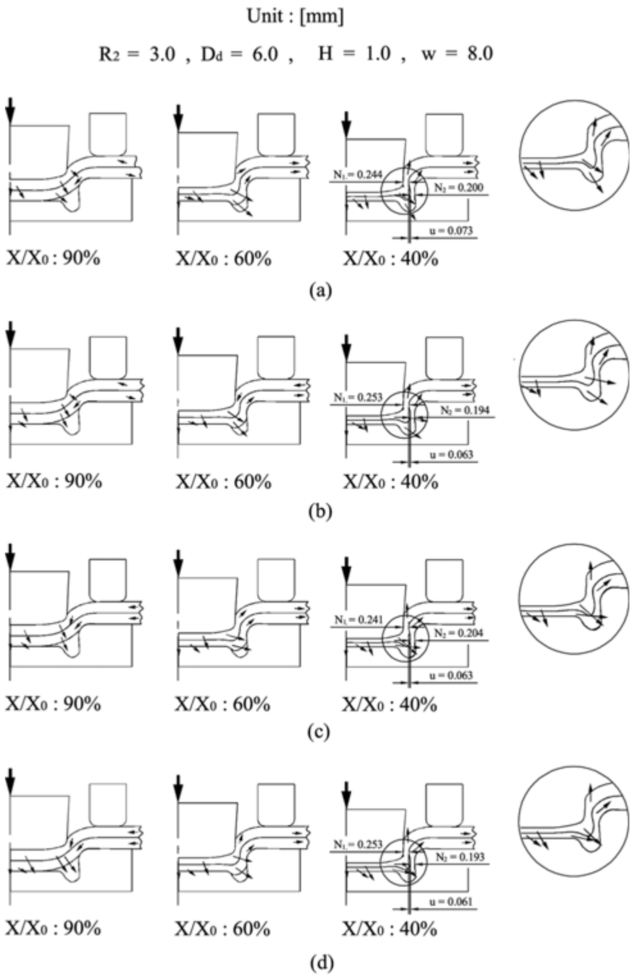

Fig. 3. Flow patterns for different FE and friction models: (a) Elastic-plastic/Coulomb, (b) Elastic-plastic/constant shear, (c) Rigid-plastic/Coulomb, and (d) Rigid-plastic/constant shear

sheets under the punch nose was about to move in the direction of the die groove, while for the rigid-plastic FE models (Figs. 3(c) and (d)), the outer periphery of the top and bottom sheets tended to flow in the direction of the center while both of the sheets under the punch flew towards the groove. When the bottom thickness (X) was reduced to 40%, the material of the outer periphery in the elastic-plastic/Coulomb model flowed outwards, whereas in the elastic-plastic/constant shear model, the top sheet changed its flow directions such that the top sheet tended to flow inward. In both rigid-plastic (Coulomb and constant shear) models, the outer periphery of the top and bottom sheets flowed simultaneously away from the center, while the radial flow intensified towards the groove. At the final stage of the clinching process, where the bottom thickness (X) was reduced up to 60%, the top sheet in the elastic-plastic/Coulomb model flowed into the groove, making a greater interlock between the two sheets than the elastic-plastic/constant shear model, where the upper sheet continued to flow in a radial direction away from the center. Also, rigid-plastic models seemed to generate better mechanical interlocking between the two sheets. However, near the die, the neck top sheet tended to flow upward, while near the groove, the bottom sheet flowed towards the die wall. This may have created counter piping (gaps) between the sheets. It seems that there was little difference in the flow patterns between the different friction models. However, the different FE models, i.e. elastic-plastic and rigid-plastic, predicted slightly different flow patterns such that a better mechanical interlocking was expected in the rigid-plastic FE model as the material flowed into the groove, but the tendency of a thinning N_1 or the formation of gaps between the sheets was higher than in the elastic-plastic FE models.

3.2. Effect of Process Parameters on Evaluation Parameters

Figure 4 shows the relationships between the die depth and u, N_1, N_2, and X, respectively, for different die diameters with 0.8 mm of w and 0.3 mm of R_2. From looking at Fig. 4(a), we can observe that the u tended to increase as the H increased and the tendency intensified a little with an increasing D_d. It can also be seen in the figure that different FE models did not influence the undercut u much for all the die diameters D_d when the die depths were between 1 mm and 1.5 mm. It is also revealed in Fig. 4(b) that N_1 tended to decrease with an increasing H and with a decreasing D_d. The FE model mostly affected the N_1 only when H was near 1.2 mm. The rigid-plastic/constant shear model seemed to show a higher N_1 for all of the die diameters applied. From the results shown in Fig. 4(c), it can be seen that N_2 was not too sensitive to the process parameters, such as H and D_d. However, as shown in Fig. 4(c), N_2 increased while D_d increased and this trend was amplified with decreasing die depths for a die diameter that was near 6.4 mm. N_2 was affected the most by FE models when the die diameter was near 5.6 mm while the FE models with Coulomb friction showed higher values for N_2 for all diameters. It is shown in Fig. 4(d) that X decreased as the die depth H and the die diameter D_d increased. It is generally known from the figure that the FE model had not much affect on X for a greater D_d. However, it is shown in Fig. 4(d) that X was the most sensitive to D_d. It is noticeable that two different FE models do not show identical results. It can be seen in Fig. 4 that the greatest values for u and N_1 and N_2 were obtained only for D_d of 6.4 mm. However, when D_d was 6.4 mm, X became too low. When D_d was near 5.6 mm, the material overfilled the die cavity such that X became greater and the values for u and necks N_1, N_2 became lower, respectively. It can be seen from the figure that the clinching process could be monitored and evaluated by examining X. The most suitable curve that satisfied the undercuts, necks, and bottom thickness was obtained for D_d

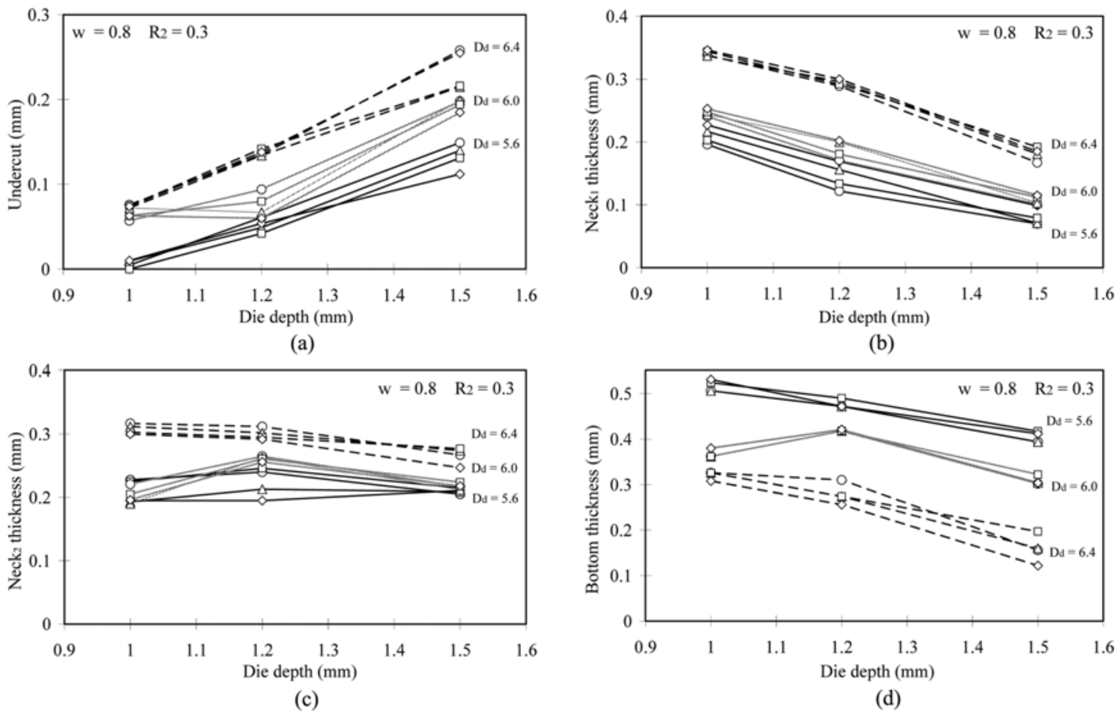

Fig. 4. Effect of die depth (H) and die diameter (D_d) on evaluation parameters.

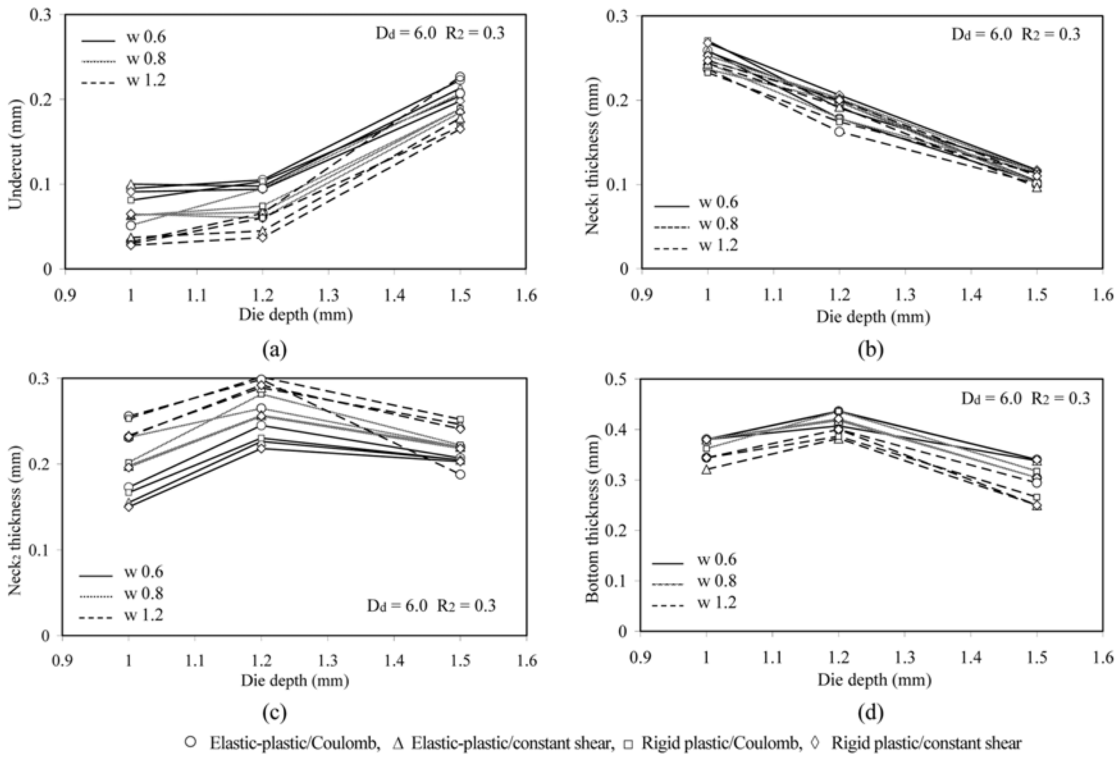

Fig. 5. Effect of die depth (H) and groove width (w) on evaluation parameters.

near 6.0 mm when H was near 1.0 mm. Also, it is important to understand from the figure that N_1 became smaller and was reduced to more than 80 % of the total sheet thickness when the die diameter was near 6 mm and the die depths were over 1.2 mm.

Extensive analysis was made on the effect of the groove width on different FE and friction models in terms of u, N_1, H and X, as shown in Fig. 5. It is easily seen in the Fig. 5(a) that the u increased as the w decreased, such that it varied gradually with the die depth between 1.0 mm and 1.2 mm. then u increased rapidly with an increasing H. The larger w tended to lead to a smaller u. The tendency was intensified with a decreasing H. The comparison of FE models showed a higher undercut u for the elastic-plastic FE models. The neck thickness of the top sheet N_1 seemed to be a little greater for a smaller w and decreased steadily with an increasing H, as shown in Fig. 5(b). The use of the rigid-plastic FE model may predict more failures of N_1. The behavior of N_2 is illustrated in Fig. 5(c) according to the variation of H. It is shown in the figure that a smaller w tended to decrease both of the neck thicknesses N_1 and N_2. The N_2 increased with a die depth between 1.0 mm and 1.2 mm, and decreased again gradually with an increasing H. The X values were not affected much by the variation of the groove width w, as shown in Fig. 5(d).

It has been known from the figures that all the evaluation parameters selected in this study had an influence on the mechanical interlocking between the construction sheets.

More extensive analyses have been made on the effect of R_2 for different FE and friction models, which are shown in Fig. 6, in terms of the relationships between H and u, N_1, N_2, and X, respectively. The effect of the groove corner radius R_2 on the evaluation parameters seemed insignificant, and even different FE models and friction models showed a similar graph.

3.3. Evaluation of Clinch Joints

The quality of clinch joint was evaluated by examining the separation strengths and they are listed in Table 2. The table shows the process conditions, evaluation parameters, and failure mode and separation strengths. The results are summarized for 5 selected cases in order to compare the evalua-

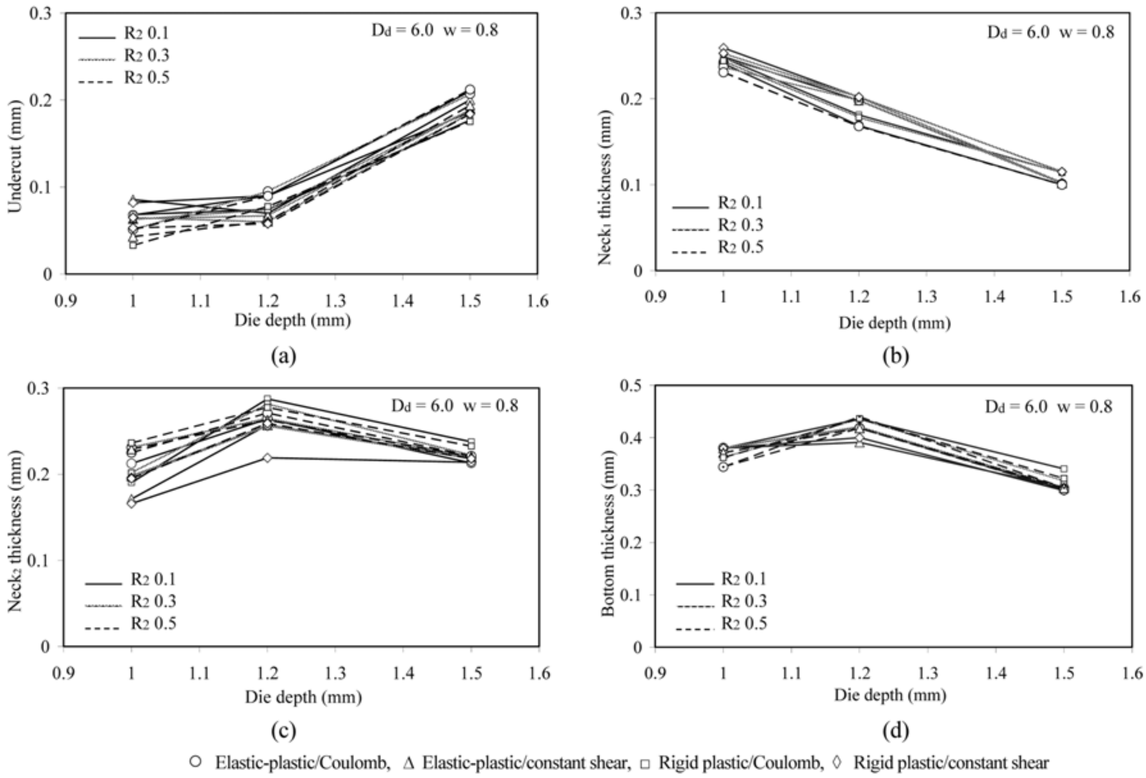

Fig. 6. Effect of die depth (H) and groove corner radius (R_2) on evaluation parameters.

Table 2. Failure modes and separation strengths (elastic-plastic/Coulomb)

Process Parameters (mm)				Evaluation parameters (mm)				Failure modes	Peel strengths (N)	Tensile-shear strengths (N)
D_d	H	w	R_2	X	u	N_1	N_2			
6.0	1.0	0.8	0.3	0.38	0.070	0.2409	0.212	Safe	110	392
6.0	1.0	0.8	0.3	0.38	(0.051)	0.237	0.231	Low (U)	83	360
6.0	1.0	0.8	0.5	(0.34)	0.051	0.231	0.225	Low (X)	55	335
6.0	1.0	0.6	0.1	0.42	0.095	(0.176)	0.240	Low (N_1)	90	360
6.0	1.0	0.6	0.3	0.38	0.095	0.259	(0.173)	Low (N_2)	107	400

tion parameters for the elastic-plastic/Coulomb friction model. It can be seen in the table that clinch joints were more resistant to the tensile shear loads than the peel off loads in detaching, as was expected. It is interesting to note that the specimen did not even show sufficient peel strength and tensile shear strengths for the "safe" case, even though N_1 and N_2 thicknesses were sufficient enough. Joints with low neck thickness seemed to be much more resistant to the detaching forces, as u was much greater than that in the first case with an undercut u of 0.07 mm. It is noticeable from the table that the u and N_1 thickness seemed to be the most important parameters for a successful clinch joint. It can also be easily understood in the table that the clinch joints could handle more peel-off loads when the X and N_1 were high. However, the most optimal tool combination was found based on the expected maximum peel-off and tensile shearing loads in separating sheets, for which X ranged from 0.38 mm and 0.42 mm. The variation of other evaluation parameters, such as N_2 and u, were not consistent for the shear strengths.

3.4. Failure Modes and Failure Diagram

Low separation strengths were induced from inadequate deformations, which were then classified into different failure modes. It is easily seen in Fig. 7 that every failure mode has distinctive material flow patterns. The material flow patterns have resulted in 6 different failure modes that were predicted by significant changes in u, N_1, N_2 and X, in the forming process of clinch joints. The failure modes included (1) formation of gap between the sheets due to insufficient penetration of the punch side sheet, as shown in Fig. 7(a), (2) insufficient undercut, as shown in Fig. 7(b), (3) insufficient neck thickness of the top sheet, as shown in Fig. 7(c), (4) insufficient neck thickness of the bottom sheet, as shown in Fig. 7(d), (5) insufficient bottom thickness, as shown in Fig. 7(e), and (6) combination failures of insufficient necks N_1 and N_2, as shown in Fig. 7(f).

The bottom thickness of clinch joints has a strong effect on the condition of mechanical interlocking between the sheets, as summarized in Table 2. Thus, it could be possible to identify a criterion based on the X in order to determine the quality of joints. It can also be seen in the figure that the best choice of process parameters for successful clinch joints could be between 1.0 mm to 1.2 mm in die depth, together with a groove corner radius ($R_2 = 0.3$). In this particular case, as proven from the simulation results, the N_1 thickness reduced when the die depth increased. Also, it was noticeable that the selected combination of process parameters that led to unsuccessful clinch joints seemed to be in the range of bottom thickness X being smaller or greater than 0.38 mm or 0.45 mm, which always produced failures in clinch joints, such as low necks N_1, N_2 and low u or gaps between the metal sheets. This means that the X could be an effective control parameter for determining safe clinching joint processes.

All of the predicted results by simulations were analyzed again in order to draw a failure diagram in terms of process parameters. A failure diagram was constructed by four process parameters into two normalized parameters, such that parameters related to the die were separated from those

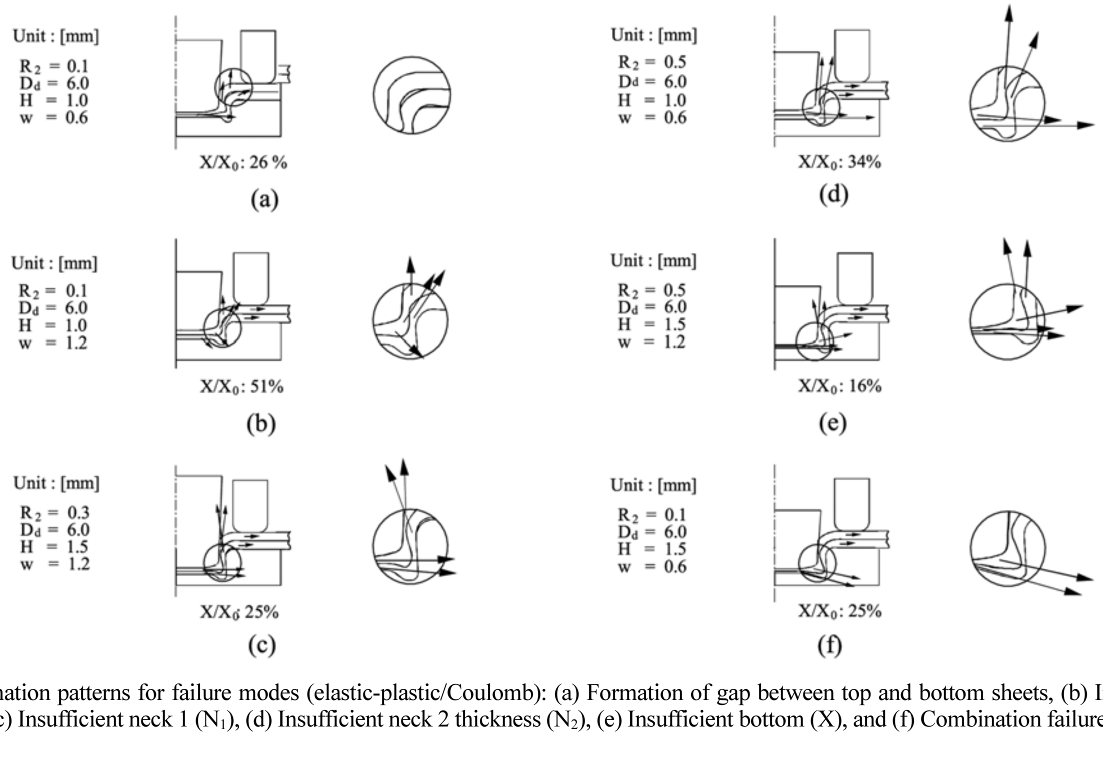

Fig. 7. Deformation patterns for failure modes (elastic-plastic/Coulomb): (a) Formation of gap between top and bottom sheets, (b) Insufficient undercut (u), (c) Insufficient neck 1 (N_1), (d) Insufficient neck 2 thickness (N_2), (e) Insufficient bottom (X), and (f) Combination failure neck (N_1) and neck (N_2).

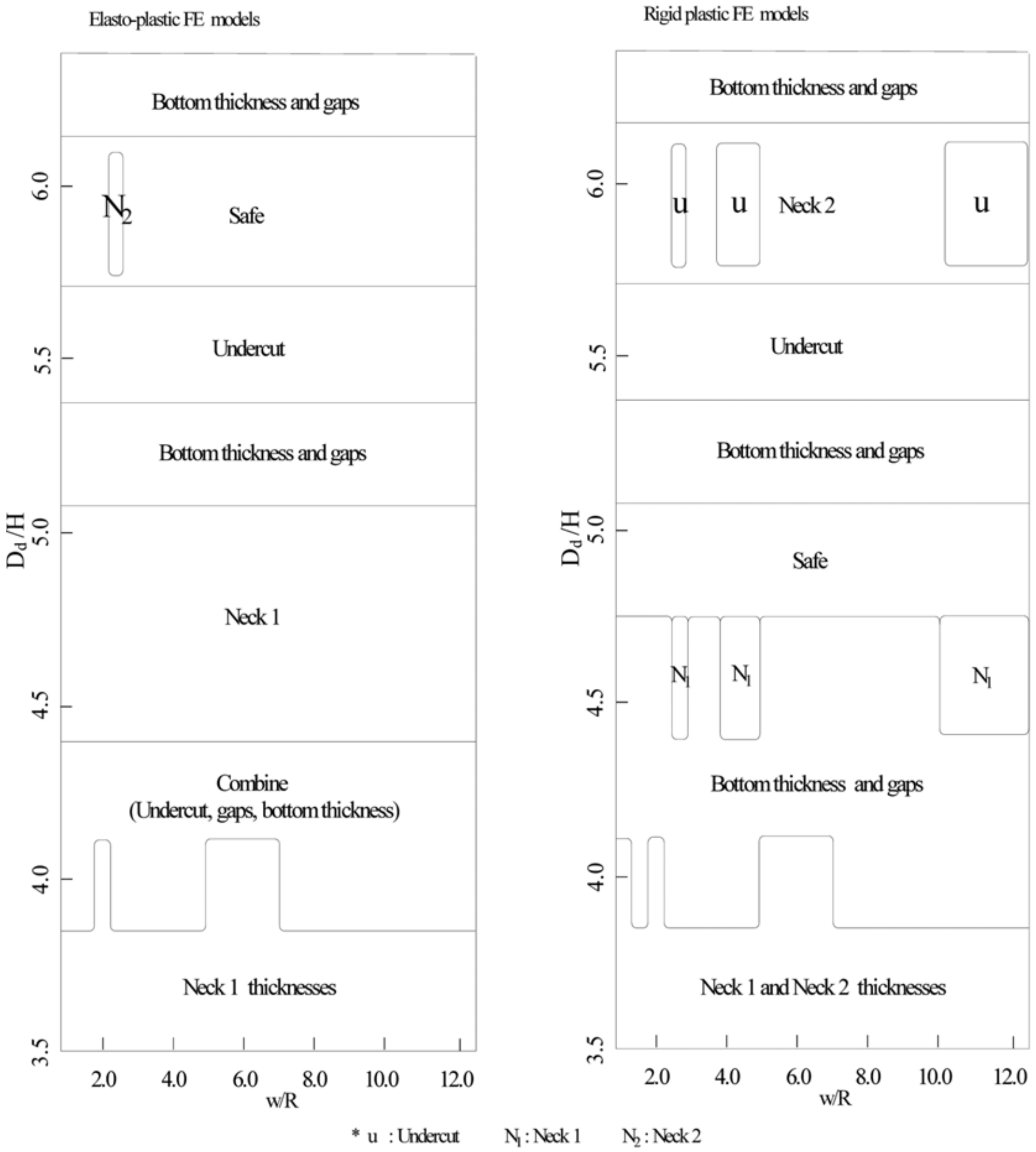

Fig. 8. Failure diagram.

related to the groove. The normalized process parameters were defined as ratio of die diameter to height (D_d/H) and that of groove width to groove corner radius (w/R_2). The failure diagram or failure map shown in Fig. 8 classifies the region of possible failures in terms of normalized process parameters. In the diagram, the safe regions were very narrow in terms of range of die parameters applied. The regions were predicted to be around 6.0 for the elastic-plastic models and around 5.0 for the rigid-plastic models, respectively. It was revealed in the diagram that the normalized parameter, (w/R_2), which is related to groove geometry, did not influence successful clinch joints, except for undercut failure. However, it can be apparently seen that the variation of die parameter, i.e. (D_d/H), led remarkably to variations in the forming patterns of the clinching process, which means that it is a very sensitive parameter to the process and could be a major, or representative, parameter for designing clinching processes.

4. CONCLUSIONS

Elastic-plastic and rigid-plastic finite element methods were applied in this study by employing laws of Coulomb friction and constant shear friction in order to analyze the clinching process of thin metal sheets. Four geometrical process parameters were considered for investigating the parametric effect on the forming process of clinching. The quality of clinch joints was evaluated by separation strengths, which were examined by the thicknesses of undercut, necks, and bottom. The failure modes were identified and a failure diagram was drawn with process parameters. The results predicted by the simulations are summarized as follows:

(1) The bottom thickness should be near the range of 40% of the original sheet thickness in order to ensure enough peel-off and tensile shearing strengths between the thin metal sheets.

(2) The bottom thickness was sensitive to the variation of die diameter and die depth. Therefore, the ratio of die diameter to height is the most decisive process parameter influencing the quality of clinch joints.

(3) The groove width and groove corner radius had little influence on evaluation parameters, such as bottom thickness, undercut, and neck thicknesses.

(4) The simulation results did not show significant difference between the two models of Coulomb friction and the constant shear friction for large deformation of thin sheet metals.

(5) The elastic-plastic and rigid-plastic finite element analysis have resulted in the ratio of die diameter to height being 6.0 and 5.0, respectively, in order to avoid the failure of clinching joints, which consisted of safe zones in the failure diagram.

(6) The ratio of die diameter to height, which is one o normalized parameters related to the die geometry, has been proven as a most decisive parameter influences on the quality of clinch joints.

ACKNOWLE DGMENT

This work was published with support of INHA UNIVERSITY Research Grant.

REFERENCES

1. J. Varis, *J. Mater. Process. Technol.* **174**, 277 (2006).
2. TOX-Pressotechnik GmbH, *Overview of TOX clinching Tech.* http://www.tox-de.com (2005).
3. J. P. Varis, *J. Mater. Process. Technol.* **132**, 242 (2003).
4. ATTEXOR Inc., *What is Clinching*, http://www.attexorinc.com (2005).
5. N. Nong, O. Keju, and Z. Yu, *J. Mater. Process. Technol.* **137**, 59 (2003).
6. M. Carboni, S. Bereetta, and M. Monno, *Eng. Fract. Mech.* **73**, 179 (2006).
7. R. F. Pedreschi, and B. P. Sinha, *Constr. Build. Mater.* **22**, 921 (2007).
8. C.-S. Chung, B.-S. Cha, and H.-K. Kim, *Mater. Manufact. Process* **16**, 387 (2001).
9. V. Hamel and J. M. Roelandt, *Comput. Struct.* **77**, 185 (2000).
10. J. Gardstam, *Licentiate thesis*, p. 5-15, Royal Institute of Technology, Sweden (2006).
11. P. Hrycaj, S. Cescotto, and J. Oudin, *J. Eng. Comput.* **8**, 291 (1991).
12. D. H. Jang and B. B Hwang, *Mater. Sci. Forum* **475**, 3255 (2005).
13. V. R. Jayasekara, J. H. Noh, B. B. Hwang, K. C. Ham, and D. H. Jang, *Trans. of Mater. Process.* **16**, 603 (2007).
14. M. Oudjene and L. Ben-Ayed, *J. Eng. Struct.* **30**, 1782 (2008).
15. P. F. Zheng, L. C. Chan, and T. C. Lee, *J. Finite Elem. Anal. Des.* **42**, 189 (2005).
16. SFTC, *DEFROM-2D Ver. 8.0 Users Manual,* Scientific Forming Technologies Corporation Inc., USA (2004).
17. J. Sarkar, T. R. G. Kutty, and K. T. Conlon, *J. Mater. Sci. Eng. A* **316**, 52 (2001).
18. H. Nordberg, *Fatigue Properties of Stainless Steel Lap Joints*, http://www.sae.org (2005).
19. A. A. de Paula, M. T. P. Aguilar, and A. E. M. Pertence, *J. Mater. Process. Technol.* **182**, 352 (2007).
20. S.-S Park, S.-M. Lee, Y.-J. Cho, *J. Kor. Inst. Met. & Mater.* **46**, 672 (2008).
21. SFTC, *DEFROM-3D Ver. 5.0 Users Manual,* Scientific Forming Technologies Corporation Inc., USA (2004).
22. Y. Tan, O. Hahn, and F. Du, *ISIJ Int.* **45**, 723 (2005).
23. J. P. Varis and J. Lepisto, *Thin-Walled Struct.* **41**, 691 (2003).
24. Adam Cort BNP Media, *In a Clinch,* http://www.assemblymag.com (2002).